Analog Equalization and Low Resolution Quantization in Strong Line-of-Sight MIMO Communication

Xiaohang Song*, Tim Hälsig†, Wolfgang Rave*, Berthold Lankl†, and Gerhard Fettweis*§

* Vodafone Chair, Technische Universität Dresden, Dresden, Germany,
Email: {xiaohang.song, wolfgang.rave, gerhard.fettweis}@tu-dresden.de
† Institute for Communications Engineering, Universität der Bundeswehr München, Germany,
Email: {tim.haelsig, berthold.lankl}@unibw.de

***Abstract*—In this work we show that the analog equalizing networks are suitable for low resolution quantization with limited mutual information loss in strong line-of-sight MIMO communication. More specifically, a simplified analog equalizing network design in comparison with state-of-the-art works is proposed in this work. Additionally, the new network design works equally good for larger displacement ranges. Furthermore, by using analog equalizing networks in line-of-sight MIMO systems, it is shown that the drawbacks of low resolution quantization can be minimized. This increases the energy efficiency of the analog-to-digital converters via minimizing the required magnitude resolution. Generally, low resolution quantization causes low entropy on the receive vectors which will effectively reduce the mutual information of the desired transmission. The analog equalizing network reshapes the distribution and reduces the dynamics of the received signals in the complex constellation plane before quantization. Therefore, the entropy loss after low resolution quantization is reduced and the system performs essentially as good as a system with higher resolutions. Finally, an algorithm is proposed to remove ambiguities which arise after analog-to-digital conversion with a given low resolution.**

I. Introduction

In 2020-2030, peak data rates in cellular networks are expected to be in the order of 10 $\mathrm{Gb/s}$ [1]. Base stations will serve multiple sectors and will be no more than 100 m apart in urban areas. Previous work [2] showed the great potential in building ultra high speed fixed wireless backhaul links to meet the growing demand for high capacity of the front/back-haul. For future dense networks, wireless front/back-haul links offer easy and cheap deployment in comparison with costly optical fibers. The unlicensed 60 GHz band has become most popular for this purpose due to available large bandwidth, high frequency reuse and reasonable array sizes which can fully exploit the spatial multiplexing gains in *Line-of-Sight* (LoS) channels. The works in [3], [4], [5] have given the solution to the optimized spatial arrangements on parallel planes that provide the MIMO channel matrices with orthogonality. However, full spatial multiplexing can also be achieved with arrangements on tilted non-parallel planes [6], [7], [8], [9] or even more complicated 3D arrangements [9]. Furthermore, [5] showed high robustness of the spatial multiplexing gain in LoS MIMO against degradations like translation and rotation. Finally, a recent idea presented in [10] shows that, with additional medium between transceiver arrays, the arrays can be more compact as the medium introduces additional optical path length.

Due to the fact that applications like wireless backhaul with LoS MIMO channels are highly deterministic, the channel parameters, as well as the equalization matrix, do not change rapidly with respect to time. Therefore, analog components can be used for channel equalization at millimeter wave frequencies. Analog equalizing networks separate the structurally interfered signals before the *Analog-to-Digital Converters* (ADCs). Works in [11], [12] demonstrated a channel equalizing network for 2×2 LoS MIMO system with phase shifters operating at intermediate frequencies. Their work was extended to a 4×4 MIMO system with variable gain amplifiers allowing magnitude scaling and phase shift operations on baseband signals [13]. The authors of [14] provide experimental evaluation of 2×2 LoS MIMO system with a fixed analog equalizing network. They intuitively point out that analog equalizing can reduce the required resolution of the ADCs without analysis and detailed study. The reason was given as the required dynamic range in multi-stream communication without stream separation networks increases along with the increase in the number of streams due to larger peak-to-average power ratios. In our work, we investigate and analyze the required amplitude resolution from a mathematical point of view. Meanwhile, a closely related work of us in [15] shows that the fixed analog equalizing network is very sensitive to displacement errors and can be further simplified into a two-stage network if uniform rectangular arrays are used.

Energy efficiency is another key performance indicator. Especially considering LoS communication, high frequencies like millimeter wave frequencies facilitate arrays of smaller sizes [2]. However, as large bandwidths have to be processed, the time resolution of the ADC has to scale correspondingly, making the converter one of the main power consumers. The resolution of ADCs should thus keep as low as possible, as the power consumption scales almost exponentially with resolution and represents a major factor in the system's energy efficiency.

The paper is organized as follows. In Section II, we introduce the system model of analog equalizing networks combined with LoS MIMO systems. In Section III, we propose

§ This work has been supported by the German Research Foundation (DFG) in the framework of priority program SPP 1655 "Wireless Ultra High Data Rate Communication for Mobile Internet Access".

978-1-4799-6664-6/16/$31.00 ©2016 IEEE

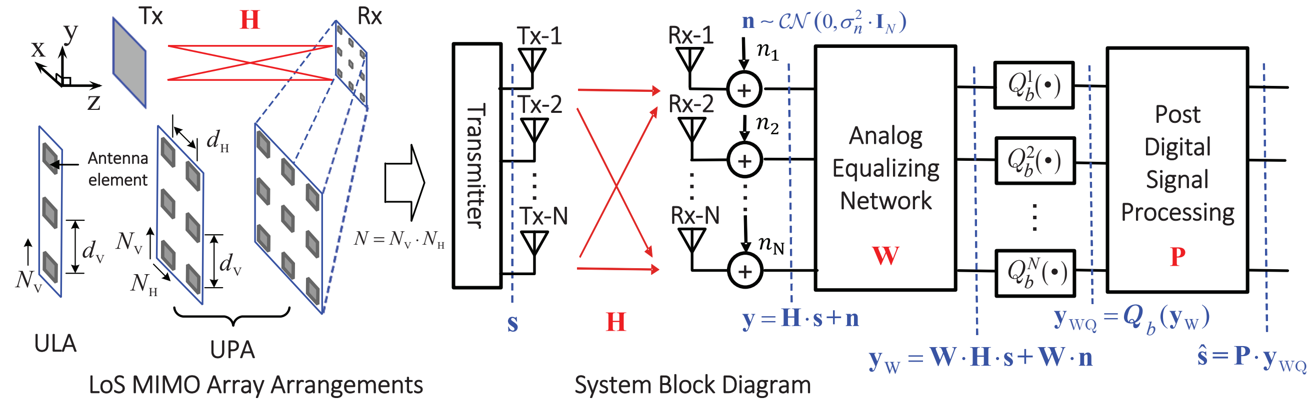

Fig. 1: System model.

a new analog equalizing network design as well as the derivation of the mutual information considering low resolution quantization. This is followed by a new algorithm that removes ambiguities arising from low resolution ADCs in Section IV. In Section V, numerical evaluations are applied to validate our claims. Finally, our work is concluded in Section VI.

II. System Model

Fig. 1 shows a symmetric $N \times N$ LoS MIMO transmission system. To simplify the description of the system, we split the system into three parts: analog equalization processing, analog-to-digital conversion, and post digital signal processing.

A. Analog Equalization

Considering a LoS MIMO system with transmit distance D which is much larger than the inter antenna distances d_{V}, d_{H}, the receive vector in a frequency flat strong LoS MIMO channel is modeled as

$$\mathbf{y} = \mathbf{H} \cdot \mathbf{s} + \mathbf{n}, \tag{1}$$

where $\mathbf{n}$ is i.i.d. zero mean complex white Gaussian noise in base-band with $\mathbf{n} \sim \mathcal{CN}(\mathbf{0}, \sigma_n^2 \cdot \mathbf{I}_N)$. $\mathbf{s}$ is the transmit vector with total transmit power P_{T}, $\mathbb{E}(\mathbf{s}^{\mathrm{H}}\mathbf{s}) \leq P_{\mathrm{T}}$. Due to the fact that the power attenuation factors between different antenna pairs are almost the same under assumption that $D >> d_{\mathrm{V}},\ d_{\mathrm{H}}$, we neglect the power differences [2]. By $\mathbf{H} \in \mathbb{C}^{N \times N}$ we denote the phase coupling matrix in the strong LoS MIMO channel with entries

$$h_{ij} \triangleq e^{-j\frac{2\pi}{\lambda}D_{ij}}, \tag{2}$$

where D_{ij} denotes the transmit distance between transmit antenna j and received antenna i. λ is the wavelength of the carrier frequency.

To simplify the later discussion, we assume that the transmitted signals in all N data streams follow the same K-QAM modulation with K constellation points $\mathbb{A} = \{\mathscr{A}_1,\ \mathscr{A}_2,\ \ldots,\ \mathscr{A}_K\}$. Therefore, the transmit vector $\mathbf{s}$ belongs to a N-dimensional discrete space $\mathbb{M} = \mathbb{A}^N$, where $\mathbb{M} = \mathbb{A}^N$ is a finite set containing all possible transmit vectors $\boldsymbol{\mathcal{S}}$s.

Considering two parallel *Uniform Linear Arrays* (ULAs) or *Uniform Planar Arrays* (UPAs) that are separated by distance D, the special arrangements following the design in [5] can fully exploit the spatial multiplexing gains of LoS MIMO systems. The arrangements and the inter antenna spacing d_{V}, d_{H} mainly depend on the transmit distance D, wavelength λ and antenna number $N = N_{\mathrm{H}} \cdot N_{\mathrm{V}}$. In symmetric cases, d_{V}, d_{H} satisfy $d_{\mathrm{V}} = \sqrt{\lambda D / N_{\mathrm{V}}}$ and $d_{\mathrm{H}} = \sqrt{\lambda D / N_{\mathrm{H}}}$, respectively. By choosing d_{V}, d_{H} appropriately and arranging the transceiver arrays in two parallel planes that are perpendicular to the transmit direction, $\mathbf{H}$ becomes the spatially orthogonal matrix $\mathbf{H}_{\mathrm{o}}$ with $\mathbf{H}_{\mathrm{o}}^{\mathrm{H}} \cdot \mathbf{H}_{\mathrm{o}} = N \cdot \mathbf{I}_N$. However, if there exists displacement of the optimal arrangement, $\mathbf{H} \neq \mathbf{H}_{\mathrm{o}}$, and the matrix is not orthogonal anymore. As an example, the entries of $\mathbf{H}_{\mathrm{o}}$ in an optimally arranged and symmetric system with ULAs satisfy $\{\mathbf{H}_{\mathrm{o}}\}_{il} = e^{-j\pi(i-l)^2/N}$. When $N = 3$, $\mathbf{H}_{\mathrm{o}}$ becomes

$$\mathbf{H}_{\mathrm{o}} = \begin{bmatrix} 1 & e^{-j\frac{\pi}{3}} & e^{-j\frac{4\pi}{3}} \\ e^{-j\frac{\pi}{3}} & 1 & e^{-j\frac{\pi}{3}} \\ e^{-j\frac{4\pi}{3}} & e^{-j\frac{\pi}{3}} & 1 \end{bmatrix}. \tag{3}$$

An analog equalizing network, represented by a weighting matrix $\mathbf{W} \in \mathbb{C}^{N \times N}$, is introduced in the system for equalizing the vector received through a deterministic MIMO channel like in a strong LoS MIMO system. The weighted vector $\mathbf{y}_{\mathrm{W}}$ is then expressed as

$$\mathbf{y}_{\mathrm{W}} = \mathbf{W} \cdot \mathbf{y} = \mathbf{W} \cdot \mathbf{H} \cdot \mathbf{s} + \tilde{\mathbf{n}}, \tag{4}$$

where $\tilde{\mathbf{n}} = \mathbf{W} \cdot \mathbf{n}$.

B. Analog-to-Digital Conversion

After equalizing the channel, the signals are quantized and converted for digital-band processing. Assuming that transceivers are perfectly synchronized, the signals are split up into real and imaginary parts. These signals are fed to the inputs of two banks of quantizers $Q^{\mathrm{R}_1}, Q^{\mathrm{R}_2}, \ldots, Q^{\mathrm{R}_N}$ for the real and $Q^{\mathrm{I}_1}, Q^{\mathrm{I}_2}, \ldots, Q^{\mathrm{I}_N}$ for the imaginary parts of different data streams $l \in \{1, 2, \ldots, N\}$. To simplify the discussion in the rest of the paper, we assume all of the above mentioned quantizers to be of the same type[1] and denoted them as $Q_b^{\alpha}(x)$ with $\alpha \in \{\mathrm{R}_1, \mathrm{R}_2, \ldots, \mathrm{R}_N\} \bigcup \{\mathrm{I}_1, \mathrm{I}_2, \ldots, \mathrm{I}_N\}$. Here,

[1] Quantizers at different data streams may not be identical to each other, if quantization are applied on signals with different scales or different distributions of amplitudes.

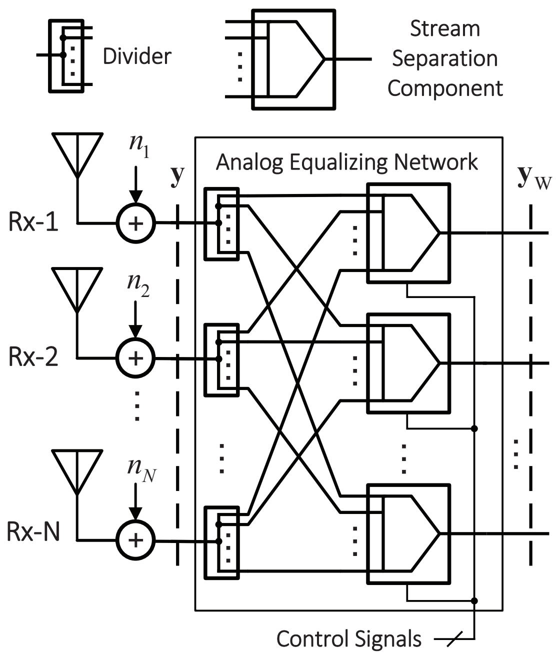

Fig. 2: Analog equalizing network block diagram.

b denotes the number of bits that are used for representing the ADC outputs. The input-output relationship $Q_b^{\alpha}(x)$ of the ADC Q^{α} is defined for voltages x by

$$Q_b^{\alpha}(x) = \begin{cases} q_1^{\alpha} & \text{if} \quad -\infty < x \leq x_1^{\alpha} \\ q_2^{\alpha} & \text{if} \quad x_1^{\alpha} < x \leq x_2^{\alpha} \\ \vdots & \vdots \qquad\qquad \vdots \\ q_{2^b}^{\alpha} & \text{if} \quad x_{2^b-1}^{\alpha} < x < +\infty \end{cases}, \tag{5}$$

where the $\{q_1^{\alpha}, q_2^{\alpha}, \ldots, q_{2^b}^{\alpha}\}$ and $\{x_1^{\alpha}, x_2^{\alpha}, \ldots, x_{2^b-1}^{\alpha}\}$ are the sets of quantization values and their thresholds, respectively.

Combining the outputs of the real and imaginary parts of the quantizers, the quantizing operation $Q_b^l(z)$ on the complex constellation plane can be written as

$$Q_b^l(z) = Q_b^{\mathrm{R}_l}[\Re(z)] + j \cdot Q_b^{\mathrm{I}_l}[\Im(z)], \tag{6}$$

where $\Re(z)$, $\Im(z)$ indicate the real and imaginary parts of the complex number z.

Now, we write the input-output relationship of the analog-to-digital conversion as

$$\mathbf{y}_{\mathrm{WQ}} = \mathbf{Q}_b(\mathbf{y}_{\mathrm{W}}) \in \mathbb{Q}, \tag{7}$$

where $\mathbb{Q}$ denotes a finite set containing all possible outputs of the quantizers.

C. Post Digital Signal Processing

If the channel is not perfectly equalized by the analog equalizing network, the vector $\mathbf{y}_{\mathrm{WQ}}$ will not be equivalent to $\mathbf{s}$ even in noise-free cases. It is reasonable to assume that the receiver has full channel state information as the channel is almost deterministic in strong LoS situations (very long coherence time). Therefore, the effective channel is $\mathbf{W} \cdot \mathbf{H}$. The post digital signal processing $\mathbf{P}$ can be applied to the quantized weighted vectors $\mathbf{y}_{\mathrm{WQ}}$ which give the estimate $\hat{\mathbf{s}}$ of transmit vectors as

$$\hat{\mathbf{s}} = \mathbf{P} \cdot \mathbf{y}_{\mathrm{WQ}}. \tag{8}$$

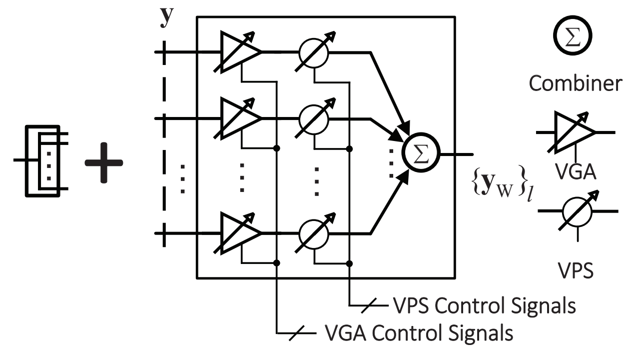

Fig. 3: Stream separation design with perfect stream equalization but complex system design. $\{\mathbf{y}_{\mathrm{W}}\}_l$ indicates the l-th element in weighted vector $\mathbf{y}_{\mathrm{W}}$.

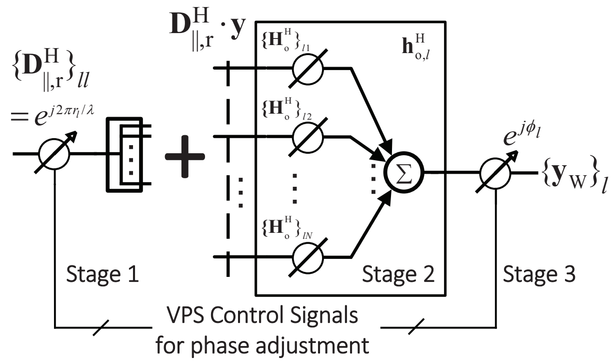

Fig. 4: Fixed stream separation with phase adjustment design.

III. Analog Equalization and Quantization

In optimal arrangements, as mentioned above, phase coupling matrices are orthogonal matrices with entries having unit modulus. Therefore, the weighting matrix $\mathbf{W}$ can be realized with entries having unit modulus, e.g. $\mathbf{W} = \mathbf{H}_{\mathrm{o}}^{\mathrm{H}}$ and $\mathbf{H}_{\mathrm{o}}^{\mathrm{H}} \cdot \mathbf{H}_{\mathrm{o}} = N \cdot \mathbf{I}_N$. Later in the discussion, the phase coupling vector for i-th transmit antenna is modeled as $\mathbf{h}_{\mathrm{o},i}$ which is the i-th column of matrix $\mathbf{H}_{\mathrm{o}}$. Considering this, the spatially orthogonal channel can be fully equalized using an analog filter network with different delays or phase shifters. The analog equalizing network constructs new weighted vectors by aligning the received signals from different receive antennas. The alignment brings performance improvement by separating one signal from the interference of the others. Therefore, the dynamics of the signals before quantization can be minimized and the required resolution can be reduced. The higher the number of antennas/amplitude levels the more quantization bits are saved by using the analog equalizer (of course the complexity of the network also grows).

The block diagram of the analog equalizing network is illustrated in Fig. 2. To simplify the diagram, we omit units for signal synchronization or carrier frequency down-conversion. We focus on the phases and amplitudes of the baseband signals. The signal from each receive antenna is split into N copies by a divider. Afterwards, every stream separation component combines the copies from all received signals. By applying different phase shifts to signals with unit magnitude, the stream separation component reconstructs the transmitted signal of the corresponding transmit antenna.

If there exists displacement of the optimal arrangement, the phase coupling matrix $\mathbf{H}$ will have mismatches with $\mathbf{H}_\mathrm{o}$, $\mathbf{H} \neq \mathbf{H}_\mathrm{o}$. In such a case, the channel could only be fully equalized using analog network components allowing arbitrary magnitude scaling and phase shifting operations. Therefore, experimental systems as in [13] used N^2 fully controlled *Variable Gain Amplifiers* (VGAs) and *Variable Phase Shifters* (VPSs) as sketched in Fig. 3 to overcome the channel mismatch. The values of the elements in $\mathbf{H}$ change rapidly with respect to small displacement. Therefore, for every different displacement in a practical system, all N^2 values need to be set differently.

A. Fixed Stream Separation with Phase Adjustment Design

As shown by P. Larsson in [5], with perfect equalization the spatial multiplexing gain is quite robust w.r.t displacement. Only under very large displacement, the undesired interferences become large and spatial multiplexing gain decreases. Therefore, having the channel perfectly equalized with very complicated hardware design and high running costs may not bring the gain worth the costs within the allowed displacements in practical systems. Hence, we suggest in this paper a fixed analog network with fewer controllable elements. The number of fully controlled VPSs is reduced from N^2 to $2N$ and it is not necessary to implement VGAs. In case of gain mismatches due to dirty RF issues, N VGAs are capable of compensating unequal amplitudes.

Considering our earlier work [9], it was shown that the phase coupling matrix can be factorized into a product of three matrices as

$$\mathbf{H} = \mathbf{D}_{\|,\mathrm{r}} \cdot \mathbf{H}_\perp \cdot \mathbf{D}_{\|,\mathrm{t}}, \tag{9}$$

where $\mathbf{D}_{\|,\mathrm{t}}$, $\mathbf{D}_{\|,\mathrm{r}}$ are diagonal matrices that represent the phase shifts caused by the offsets along the transmit direction at transmitter and receiver respectively. Their diagonal elements are $\{\mathbf{D}_{\|,\mathrm{t}}\}_{ii} \triangleq e^{j\frac{2\pi t_i}{\lambda}}$, $\{\mathbf{D}_{\|,\mathrm{r}}\}_{ll} \triangleq e^{-j\frac{2\pi r_l}{\lambda}}$, $i,l \in [1,N]$. t_i, r_l are the distances away from the planes that are passing the phase centers of transmitter and receiver respectively, and that are perpendicular to transmission direction. The matrix $\mathbf{D}_{\|,\mathrm{r}}$ introduces different phase offsets to received signals at different receive antennas and needs to be compensated for robustness purposes. $\mathbf{H}_\perp$ is the channel matrix determined by the spatial arrangement on the broadside relative to the transmit direction and $\mathbf{H}_\perp$ is also not necessarily equal to $\mathbf{H}_\mathrm{o}$. $\mathbf{H}_\perp = \mathbf{H}_\mathrm{o}$ only holds if the arrays are optimally arranged. Furthermore, the transceiver arrays are not necessary to be parallel. The arrays can be arranged on any arbitrary rotated planes or even arranged with 3D structures. The phase coupling matrices $\mathbf{H}$ will still be spatially orthogonal with arrangements shown in [9] and $\mathbf{H}_\perp$ of $\mathbf{H}$ equals to $\mathbf{H}_\mathrm{o}$.

The proposed stream separation components consist of three stages as shown in Fig. 4 for a single data stream l. The first stage applies phase shifts before the divider and compensates $\mathbf{D}_{\|,\mathrm{r}}$ caused by displacements in transmit direction for better robustness. The second stage consists of a fixed stream separation component $\mathbf{f}_l^\mathrm{T} = \mathbf{h}_{\mathrm{o},l}^\mathrm{H}$ with fixed phase shifters or delay lines that can perfectly separate the l-th channel in case of optimal arrangements. The third stage consists of a VPS with phase shift ϕ_l. The VPS compensates the remaining phase shift on the desired signal. In case of an optimal antenna arrangement with parallel antenna arrays, $\mathbf{f}_l^\mathrm{T} \cdot \mathbf{h}_{\mathrm{o},i} = N \cdot \delta_{il}$ and $\phi_l = 0$, whereδ_{il} indicates the Kronecker delta.

Considering displacements of the optimal arrangements involving translations and rotations, the phase coupling $\mathbf{H}_\perp$ is different from $\mathbf{H}_\mathrm{o}$ by $\Delta\mathbf{H}$ and therefore the channel matrix $\mathbf{H}$ is modeled as

$$\mathbf{H} = \mathbf{D}_{\|,\mathrm{r}} \cdot \underbrace{(\mathbf{H}_\mathrm{o} + \Delta\mathbf{H})}_{\mathbf{H}_\perp} \cdot \mathbf{D}_{\|,\mathrm{t}}. \tag{10}$$

The filtered signal of the l-th data steam after analog filtering satisfies

$$\begin{aligned} y_{\mathrm{F},l} &= \mathbf{f}_l^\mathrm{T} \cdot \mathbf{D}_{\|,\mathrm{r}}^\mathrm{H} \cdot \mathbf{y} \\ &= \mathbf{f}_l^\mathrm{T} \cdot [(\mathbf{H}_\mathrm{o} + \Delta\mathbf{H}) \cdot \mathbf{D}_{\|,\mathrm{t}} \cdot \mathbf{s} + \mathbf{D}_{\|,\mathrm{r}}^\mathrm{H} \cdot \mathbf{n}] \\ &= (N \cdot \mathbf{e}_l^\mathrm{T} + \mathbf{f}_l^\mathrm{T} \cdot \Delta\mathbf{H}) \cdot \mathbf{D}_{\|,\mathrm{t}} \cdot \mathbf{s} + \mathbf{f}_l^\mathrm{T} \cdot \mathbf{D}_{\|,\mathrm{r}}^\mathrm{H} \cdot \mathbf{n} \\ &= \underbrace{(N + \mathbf{f}_l^\mathrm{T} \cdot \Delta\mathbf{h}_l) \cdot e^{j\frac{2\pi t_l}{\lambda}} \cdot s_l}_{\text{Desired signal}} + \underbrace{\sum_{p=1,p\neq l}^{N} \mathbf{f}_l^\mathrm{T} \cdot \Delta\mathbf{h}_p \cdot e^{j\frac{2\pi t_p}{\lambda}} \cdot s_p}_{\text{Undesired Interference}} \\ &\quad + \underbrace{\mathbf{f}_l^\mathrm{T} \cdot \mathbf{D}_{\|,\mathrm{r}}^\mathrm{H} \cdot \mathbf{n}}_{\text{Noise}}, \end{aligned} \tag{11}$$

where $\Delta\mathbf{h}_p$ corresponds to the p-th column of $\Delta\mathbf{H}$ and $\mathbf{e}_l$ is the basis vector with the l-th element 1 and others 0.

Considering the dominant part of the filtered signal, the desired signal part has phase offset due to $\mathbf{f}_l^\mathrm{T} \cdot \Delta\mathbf{h}_l$ and $e^{j\frac{2\pi t_l}{\lambda}}$. However, the phase offset on the constellation plane can be compensated by a VPS in the third stage or a phase-locked loop during a training process. We have the phase shift ϕ_l in the third stage as

$$\phi_l = -\arctan\left\{ \frac{\Im[(N + \mathbf{f}_l^\mathrm{T} \cdot \Delta\mathbf{h}_l) \cdot e^{j\frac{2\pi t_l}{\lambda}}]}{\Re[(N + \mathbf{f}_l^\mathrm{T} \cdot \Delta\mathbf{h}_l) \cdot e^{j\frac{2\pi t_l}{\lambda}}]} \right\}. \tag{12}$$

Therefore, the weighting matrix $\mathbf{W}$ is modeled as

$$\mathbf{W} = \mathbf{\Phi} \cdot \mathbf{H}_\mathrm{o}^\mathrm{H} \cdot \mathbf{D}_{\|,\mathrm{r}}^\mathrm{H}, \tag{13}$$

where $\mathbf{\Phi}$ is a diagonal matrix with $\mathbf{\Phi} = \mathrm{diag}\{e^{j\phi_1},\ e^{j\phi_2}, \cdots,\ e^{j\phi_N}\}$.

B. Mutual Information with Quantization

In this part, we show the potential of using analog equalizing networks for reducing the required resolution of quantizers in LoS MIMO systems. Due to the fact that the displacement introduces undesired interferences to streams and in order to evaluate the performance, we use mutual information as our measure for the performance evaluation. To compare the system with and without equalizing network, based on the receive vectors $\mathbf{y}$ and $\mathbf{y}_{\mathrm{W}}$ before and after equalization, we consider their respective quantized versions $\mathbf{y}_{\mathrm{WQ}}$, as defined in Section II and the quantized receive vector $\mathbf{y}_{\mathrm{Q}}$, defined as

$$\mathbf{y}_{\mathrm{Q}} = \mathbf{Q}_b(\mathbf{y}). \tag{14}$$

The symbol $I(\mathbf{s};\mathbf{y}_{\mathrm{Q}})$ denotes the mutual information between the transmit vector and the receive vector defined in the standard way by a difference of unconditional and conditional entropy as

$$I(\mathbf{s};\mathbf{y}) = H(\mathbf{s}) - H(\mathbf{s}|\mathbf{y}). \tag{15}$$

The mutual information $I_b(\mathbf{s},\mathbf{y}_{\mathrm{WQ}})$ between $\mathbf{s}$ and $\mathbf{y}_{\mathrm{WQ}}$ with ADC resolution of b-bits is expressed as

$$I_b(\mathbf{s};\mathbf{y}_{\mathrm{WQ}}) = H(\mathbf{s}) - H(\mathbf{s}|\mathbf{y}_{\mathrm{WQ}}). \tag{16}$$

As quantization noise is introduced in the process of quantization, it is clear that $H(\mathbf{s}|\mathbf{y}_{\mathrm{WQ}}) \geq H(\mathbf{s}|\mathbf{y})$ and $I_b(\mathbf{s};\mathbf{y}_{\mathrm{WQ}}) \leq I(\mathbf{s};\mathbf{y})$.

Now let us compare the mutual information of $I_b(\mathbf{s},\mathbf{y}_{\mathrm{WQ}})$ with $I_b(\mathbf{s},\mathbf{y}_{\mathrm{Q}})$ when the channel matrix $\mathbf{H}$ is assumed to be perfectly known. Equation (16) can be rewritten as

$$\begin{aligned} I_b(\mathbf{s};\mathbf{y}_{\mathrm{WQ}}) &= H(\mathbf{y}_{\mathrm{WQ}}) - H(\mathbf{y}_{\mathrm{WQ}}|\mathbf{s}) \\ &= H(\mathbf{y}_{\mathrm{WQ}}) - H\big[\mathbf{Q}_b(\mathbf{W}\cdot\mathbf{H}\cdot\mathbf{s}+\tilde{\mathbf{n}})|\mathbf{s}\big], \end{aligned} \tag{17}$$

while $I_b(\mathbf{s},\mathbf{y}_{\mathrm{Q}})$ is expressed as

$$\begin{aligned} I_b(\mathbf{s};\mathbf{y}_{\mathrm{Q}}) &= H(\mathbf{y}_{\mathrm{Q}}) - H(\mathbf{y}_{\mathrm{Q}}|\mathbf{s}) \\ &= H(\mathbf{y}_{\mathrm{Q}}) - H\big[\mathbf{Q}_b(\mathbf{H}\cdot\mathbf{s}+\mathbf{n})|\mathbf{s}\big]. \end{aligned} \tag{18}$$

Due to the non-linearity of the quantizing operation, the values of $H(\mathbf{y}_{\mathrm{WQ}}|\mathbf{s})$ and $H(\mathbf{y}_{\mathrm{Q}}|\mathbf{s})$ are difficult to evaluate. However, as we are focusing on the effects that are caused by using analog equalizing network and quantizers, we consider the noise-free case (high SNR limit) for which it holds that $H(\mathbf{y}_{\mathrm{WQ}}|\mathbf{s}) = H(\mathbf{y}_{\mathrm{Q}}|\mathbf{s}) = 0$.

The analog equalizing network may reshape the distribution of the constellations on the complex constellation plane of every data stream before the quantization. Therefore a weighting matrix $\mathbf{W}$ is capable of increasing the entropy of the quantized weighted vector $\mathbf{y}_{\mathrm{WQ}}$ and making $H(\mathbf{y}_{\mathrm{WQ}}) \geq H(\mathbf{y}_{\mathrm{Q}})$. Considering Equation (17) and (18), the analog equalizing network can potentially generate $I_b(\mathbf{s};\mathbf{y}_{\mathrm{WQ}}) \geq I_b(\mathbf{s};\mathbf{y}_{\mathrm{Q}})$. Due to the fact that after quantization, several different transmit vectors $\mathbf{s}$ can be mapped to the same quantized output $\mathbf{y}_{\mathrm{WQ}}$, not all the transmit vectors in $\mathbb{M}$ should be used. Therefore, the capacities C_{WQ} of the proposed system and C_{Q} of the system without analog equalization can be obtained by optimizing the probability mass function $p_{\mathbf{s}}(\boldsymbol{\mathcal{S}})$ of different transmit vectors with $\mathcal{S} \in \mathbb{M}$ via

$$C_{\mathrm{WQ}} = \max_{p_{\mathbf{s}}(\boldsymbol{\mathcal{S}})} I_b(\mathbf{s};\mathbf{y}_{\mathrm{WQ}}), \tag{19}$$

$$C_{\mathrm{Q}} = \max_{p_{\mathbf{s}}(\boldsymbol{\mathcal{S}})} I_b(\mathbf{s};\mathbf{y}_{\mathrm{Q}}). \tag{20}$$

In Section V we also would like to compare the mutual information of the proposed system with N independent and identically distributed streams. Assuming that all possible transmit vectors have equal probabilities with $p_{\mathbf{s}}(\boldsymbol{\mathcal{S}}) = 1/|\mathbb{M}| = (1/K)^N$, $\boldsymbol{\mathcal{S}} \in \mathbb{M}$, the achievable rates of the system can be numerically evaluated as

$$R_{\mathrm{WQ}} = I_b(\mathbf{s};\mathbf{y}_{\mathrm{WQ}}),\ \text{s.t.}\ \forall\boldsymbol{\mathcal{S}},\ p_{\mathbf{s}}(\boldsymbol{\mathcal{S}}) = 1/|\mathbb{M}|, \tag{21}$$

$$R_{\mathrm{Q}} = I_b(\mathbf{s};\mathbf{y}_{\mathrm{Q}}),\ \text{s.t.}\ \forall\boldsymbol{\mathcal{S}},\ p_{\mathbf{s}}(\boldsymbol{\mathcal{S}}) = 1/|\mathbb{M}|. \tag{22}$$

IV. Ambiguity Removal Algorithm

By examining Equation (19) and (20), the probability of the transmit vector $\boldsymbol{\mathcal{S}}$ within a finite transmit vector set $\mathbb{M}$ should be optimized to achieve the capacity. However, coarse quantization may lead to ambiguity of the transmit vectors. The definition of coarse quantization was given in [16]. We repeat it for the sake of completeness.

Definition 1. *A quantization scheme is called* **coarse** *iff*

$$\exists(\boldsymbol{\mathcal{S}}_1, \boldsymbol{\mathcal{S}}_2 \neq \boldsymbol{\mathcal{S}}_1) \in \mathbb{M} \quad : \quad \mathbf{Q}(\mathbf{y}_{\boldsymbol{\mathcal{S}}_1}) = \mathbf{Q}(\mathbf{y}_{\boldsymbol{\mathcal{S}}_2}), \tag{23}$$

where $\mathbf{y}_{\boldsymbol{\mathcal{S}}_1}$ *and* $\mathbf{y}_{\boldsymbol{\mathcal{S}}_2}$ *are the zero-noise receive vectors corresponding to the transmit vector* $\boldsymbol{\mathcal{S}}_1$ *and* $\boldsymbol{\mathcal{S}}_2$*, respectively. Otherwise, it is said to be* **non-coarse***.*

Due to the fact that not all possible transmit vectors are distinguishable from the others in a coarse-quantization system, even if the noise power is reduced to zero, not all possible transmit vectors are necessary. The second perspective is maximizing the minimum Euclidean distance of the constellation diagram, in order to improve the robustness against noise. Therefore we develop **Algorithm 1** to determine the most effective transmit vector set $\mathbb{M}_{\mathrm{e}}$ and remove the coarseness if it exists.

Algorithm 1: Ambiguity Removal Algorithm

Input: $\mathbf{W}\cdot\mathbf{H}$ (or $\mathbf{H}$), $\mathbb{M}$, quantizer Type and b

Output: $\mathbb{M}_{\mathrm{e}}$, $\mathbf{Q}_b(\mathbf{z})$

1 Initializing quantizer:

(I) $\forall\boldsymbol{\mathcal{S}} \in \mathbb{M}$, calculate the noise free signals before quantization

$$\mathbf{y}_{\boldsymbol{\mathcal{S}}} = \begin{cases} \mathbf{W}\cdot\mathbf{H}\cdot\boldsymbol{\mathcal{S}} & \text{for weighted vectors,} \\ \mathbf{H}\cdot\boldsymbol{\mathcal{S}} & \text{for receive vectors without } \mathbf{W}. \end{cases}$$

(II) Based on all possible constellations $\mathbf{y}_{\boldsymbol{\mathcal{S}}}$s before quantization, quantizer type and b, set quantization values and thresholds for $\mathbf{Q}_b(\mathbf{z})$.

2 Finding Ambiguity:

(I) Initialize $\mathbb{Q}$ with $\mathbb{Q} = \{\mathbf{q}\big|\mathbf{q} = \mathbf{Q}_b(\mathbf{y}_{\boldsymbol{\mathcal{S}}}), \forall\boldsymbol{\mathcal{S}} \in \mathbb{M}\}$.

(II) $\forall\mathbf{q}_i \in \mathbb{Q}$ finding $\mathbb{S}_i = \{\boldsymbol{\mathcal{S}}\big|\|\mathbf{q}_i - \mathbf{Q}_b(\boldsymbol{\mathcal{S}})\|_2 = 0, \forall\boldsymbol{\mathcal{S}} \in \mathbb{M}\}$.

3 Remove Ambiguity:

(I) Finding unique transmit vectors

$$\boldsymbol{\mathcal{S}}_i : \arg\min_{\boldsymbol{\mathcal{S}}\in\mathbb{S}_i} \|\mathbf{y}_{\boldsymbol{\mathcal{S}}} - \mathbf{q}_i\|_2.$$

(II)Define the effective transmit vector set

$$\mathbb{M}_{\mathrm{e}} = \cup\{\boldsymbol{\mathcal{S}}_i\}.$$

V. Simulation and Numerical Results

There exists two kinds of degradations to the system performance, interference caused by the displacement and thermal noise. In this section, we will evaluate the system robustness with respect to those two degradations, system performance versus *Signal-to-Noise Ratio* (SNR) and *Interference* caused by displacements.

Considering optimally arranged systems, under different SNRs, the undesired interference signals in Equation (11) vanish. In Fig. 5 we show the normalized mutual information for optimal (orthogonal channel matrix) two and three antenna MIMO systems with and without the analog equalizing network and for different quantization resolutions. For this evaluation we employ 16-QAM signaling, a uniform quantization and a quantization range that is equal to the maximally possible received symbols at the ADC inputs without noise. The results reveal a couple of interesting facts. For the 1-bit quantization case the maximum achievable rate, limited by the quantizer to 2 *Bits Per Channel Use per antenna* (BPCU per antenna), is achieved when using the analog equalizer. Without this analog network the mutual information is lower and a higher resolution will be required in order to achieve the same performance. For higher resolutions the maximum achievable rate of 16-QAM, which is 4 BPCU per antenna, is always achieved when using the analog equalizer. The mutual information of the system not employing an analog receiver is clearly lower in all cases, meaning that in order to achieve the same performance a converter with higher resolution has to be chosen, e.g., in the two antenna case 1-bit of amplitude resolution can be saved at high SNRs. The number of resolution bits that can be saved depends on the dimensions of the system, i.e., size of modulation alphabet and number of antennas. Due to the central limit theorem, the received constellation will be more Gaussian like if larger values appear in the above mentioned two dimensions. This leads to larger variances and larger dynamic ranges. Therefore, higher resolutions are required for systems without analog equalization.

The undesired interference in Equation (11) is caused by displacements of the antenna arrangement. Therefore, an evaluation is carried out for the input constrained mutual information of the displaced systems in the noise-free case. As suggested by [5], the displacement errors of the system in Fig. 1 for optimal arranged LoS MIMO are categorized into four kinds which are

- Translation error in transmit direction (z-axis)
- Translation error in the y-axis of the ULAs or x-(or y-) axis of UPAs
- Rotation error around the transmit direction (z-axis)
- Rotation error around x-(or y-) axis.

As shown in [5], even at a high SNR like 20 dB, displacements should be limited in certain ranges such that the systems can achieve reasonable spatial multiplexing gains. Considering practical systems, a specific antenna arrangement design should be capable of providing service in certain ranges

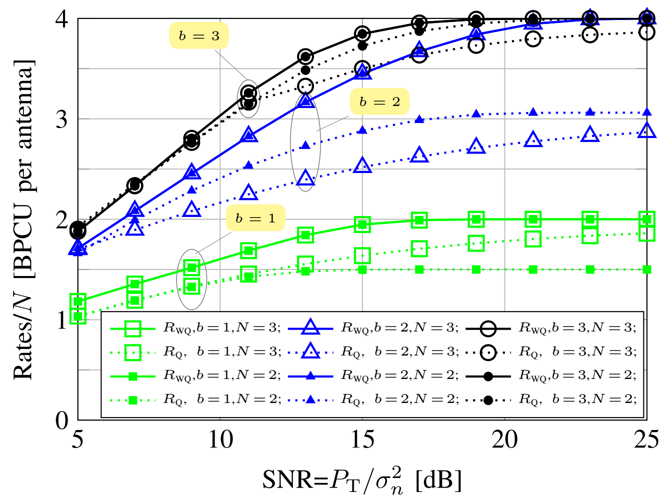

Fig. 5: Mutual Information per antenna for different SNRs. Evaluations are applied with modulation scheme 16-QAM, uniform quantizers, and $\mathbf{H} = \mathbf{H}_{\mathrm{o}}$.

with limited performance loss. Numerical evaluations of the above mentioned four kinds of displacement are carried out with 16-QAM, uniform quantizers, $N = 3$, $D = 100$ m, carrier frequency of 60 GHz, and are shown in Fig. 6-9. The system performance with analog equalization C_{WQ}, R_{WQ} always outperform the systems without analog equalization C_{Q}, R_{Q}. When considering quantization resolutions of the same level as the modulation ($b = 2$), it is seen that the capacity C_{WQ} and mutual information R_{WQ} achieve the maximum rate of 4 bits per stream while C_{Q} and R_{Q} attain only some 70%∼80% of it for all cases. Note, however, that the performance of the unequalized system could also be improved, if we would increase the number of quantization bits, e.g. $b = 3$. Finally, by using the proposed ambiguity removal algorithm, the mutual information loss due to large displacements, the ambiguities of quantized vectors without analog equalization or enough resolution can both be minimized (comparing larger markers with smaller ones).

VI. Conclusion

In this paper, we firstly showed that it is not necessary to use the conventional analog equalizing networks in strong LoS MIMO systems with displacements, via proposing a much simplified analog equalizing network design. Secondly, we showed that it is possible to keep the resolution of the quantizers at the same level as required by the modulation alphabet. This simplification is achieved by employing an analog equalizing network. Keeping the quantization resolution low for the purpose of energy efficient ADCs, the system is still very robust and can perform as good as a conventional digitally equalized system with higher quantization resolution. Thirdly, by an optimization of the effective transmit vectors with the proposed ambiguity removal algorithm, the loss of the mutual information can be minimized if large displacements appear in practical systems.

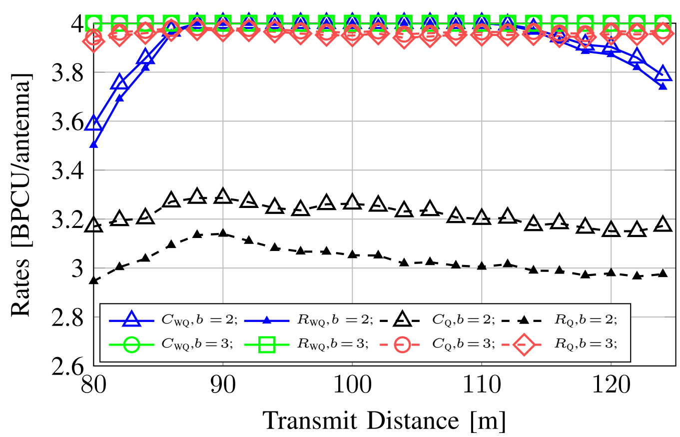

Fig. 6: Translation error in transmit direction (z-axis).

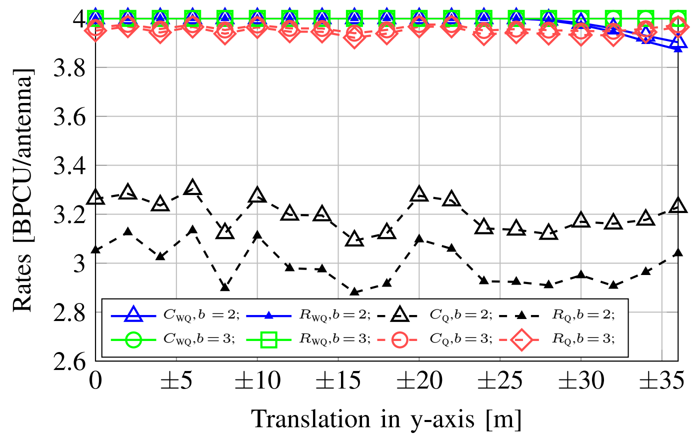

Fig. 7: Translation error in the y-axis.

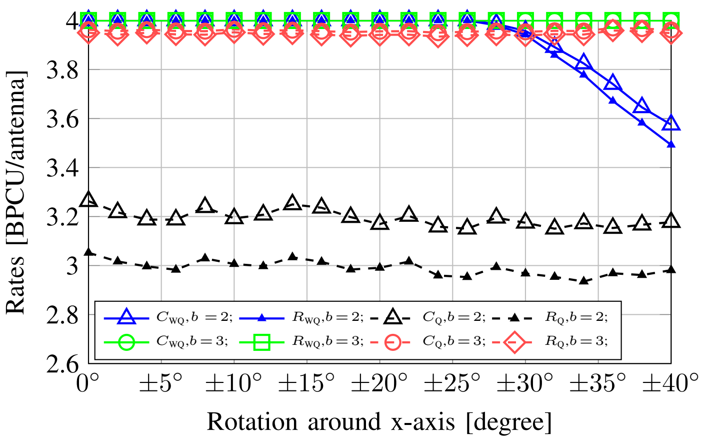

Fig. 8: Rotation error around x-axis.

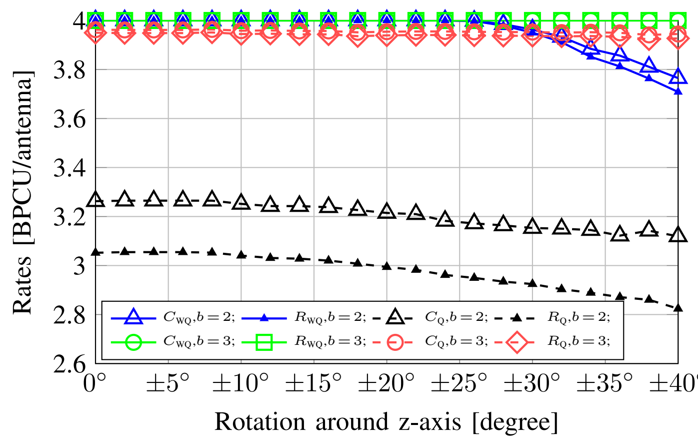

Fig. 9: Rotation error around z-axis.

References

[1] G. Fettweis, "LTE: The Move to Global Cellular Broadband," *Intel Technical Journal, special issue on LTE*, vol. 18, pp. 7–10, Feb 2014.

[2] X. Song, C. Jans, L. Landau, D. Cvetkovski, and G. Fettweis, "A 60GHz LOS MIMO Backhaul Design Combining Spatial Multiplexing and Beamforming for a 100Gbps Throughput," in *Proceedings of the IEEE Global Communications Conference*, Dec 2015.

[3] D. Gesbert, H. Bolcskei, D. Gore, and A. Paulraj, "Outdoor MIMO Wireless Channels: Models and Performance Prediction," *IEEE Transactions on Communications*, vol. 50, no. 12, pp. 1926–1934, Dec 2002.

[4] T. Haustein and U. Kruger, "Smart Geometrical Antenna Design Exploiting the LOS Component to Enhance a MIMO System Based on Rayleigh-fading in Indoor Scenarios," in *Proceedings of the IEEE International Symposium on Personal, Indoor and Mobile Radio Communications*, vol. 2, Sep 2003, pp. 1144–1148.

[5] P. Larsson, "Lattice Array Receiver and Sender for Spatially Orthonormal MIMO Communication," in *Proceedings of the IEEE 61st Vehicular Technology Conference*, vol. 1, May 2005, pp. 192–196.

[6] F. Bohagen, P. Orten, and G. Oien, "Construction and Capacity Analysis of High-rank Line-of-sight MIMO Channels," in *Proceedings of the IEEE Wireless Communications and Networking Conference*, vol. 1, March 2005, pp. 432–437.

[7] ——, "Optimal Design of Uniform Planar Antenna Arrays for Strong Line-of-Sight MIMO Channels," in *Proceedings of the IEEE Workshop on Signal Processing Advances in Wireless Communications*, July 2006, pp. 1–5.

[8] C. Zhou, X. Chen, X. Zhang, S. Zhou, M. Zhao, and J. Wang, "Antenna Array Design for LOS-MIMO and Gigabit Ethernet Switch-Based Gbps Radio System," *International Journal of Antennas and Propagation*, 2012.

[9] X. Song and G. Fettweis, "On Spatial Multiplexing of Strong Line-of-Sight MIMO With 3D Antenna Arrangements," *IEEE Wireless Communications Letters*, vol. 4, no. 4, pp. 393–396, Aug 2015.

[10] T. Halsig and B. Lankl, "Array Size Reduction for High-Rank LOS MIMO ULAs," *IEEE Wireless Communications Letters*, vol. 4, no. 6, pp. 649–652, Dec 2015.

[11] C. Sheldon, E. Torkildson, M. Seo, C. Yue, U. Madhow, and M. Rodwell, "A 60GHz Line-of-sight 2x2 MIMO Link Operating at 1.2Gbps," in *Proceedings of the IEEE International Antennas and Propagation Society Symposium*, July 2008.

[12] C. Sheldon, E. Torkildson, M. Seo, C. Yue, M. Rodwell, and U. Madhow, "Spatial Multiplexing over a Line-of-Sight Millimeter-wave MIMO Link: A Two-Channel Hardware Demonstration at 1.2Gbps over 41m Range," in *Proceedings of European Conference on Wireless Technology*, Oct 2008, pp. 198–201.

[13] C. Sheldon, M. Seo, E. Torkildson, M. Rodwell, and U. Madhow, "Four-channel Spatial Multiplexing over a Millimeter-Wave Line-of-Sight Link," in *Proceedings of the IEEE MTT-S International Microwave Symposium Digest*, June 2009, pp. 389–392.

[14] K. Hiraga, K. Sakamoto, T. Seki, T. Tsubaki, H. Toshinaga, and T. Nakagawa, "Performance Measurement of Broadband Simple Decoding in Short-Range MIMO," in *Proceedings of the IEEE International Symposium on Personal, Indoor and Mobile Radio Communications*, Sep 2014, pp. 213–216.

[15] X. Song, W. Rave, and G. Fettweis, "Analog and Successive Channel Equalization in Strong Line-of-Sight MIMO Communication," in *Proceeding of IEEE International Conference on Communications*, May 2016.

[16] J. A. Nossek and M. T. Ivrlač, "Capacity and Coding for Quantized MIMO Systems," in *Proceedings of the International Conference on Wireless Communications and Mobile Computing*, 2006, pp. 1387–1392, (invited).